



Cite this: DOI: 10.1039/c7cy02167d

Transfer hydrogenation of nitrogen heterocycles using a recyclable rhodium catalyst immobilized on bipyridine-periodic mesoporous organosilica†

Kazuma Matsui,^a Yoshifumi Maegawa,^b Minoru Waki,^b
Shinji Inagaki*^b and Yoshihiko Yamamoto *^a

Transfer hydrogenation of unsaturated nitrogen heterocycles using a rhodium catalyst immobilized on bipyridine-periodic mesoporous organosilica (BPy-PMO) is described. The immobilized catalyst was prepared by mixing $[\text{Cp}^*\text{RhCl}_2]_2$ ($\text{Cp}^* = \eta^5\text{-C}_5\text{Me}_5$) with BPy-PMO powder in DMF at 60 °C and characterized by nitrogen adsorption measurements, solid-state NMR spectroscopy, X-ray diffraction, energy-dispersive X-ray spectroscopy, and transmission electron microscopy. In the presence of the catalyst, a wide variety of unsaturated nitrogen heterocycles underwent transfer hydrogenation to afford the corresponding products in good yields. The immobilized catalyst could be readily recovered by centrifugation and reused several times in the transfer hydrogenation process.

Received 21st October 2017,
Accepted 6th December 2017

DOI: 10.1039/c7cy02167d

rsc.li/catalysis

Introduction

Saturated nitrogen heterocycles are ubiquitous in natural products and drug molecules.¹ Therefore, a variety of methods have been developed for the synthesis of saturated nitrogen heterocycles.^{1d,2} Among these, hydrogenation of unsaturated heterocycles has been recognized as a straightforward route to saturated heterocycles.^{1d,3} Moreover, transfer hydrogenation has a practical advantage over conventional hydrogenation in that safe and inexpensive hydrogen donors can be utilized instead of hydrogen gas.⁴ Thus, transfer hydrogenation circumvents the use of pressure equipment. Although transfer hydrogenation of unsaturated nitrogen heterocycles has been realized using homogeneous catalysts,^{1d,3} the application of such catalysts to the production of fine chemicals is still limited because of the difficulties in catalyst separation and recycling. Therefore, the development of a high-performance recyclable catalyst for transfer hydrogenation is of great importance. Nevertheless, the substrate scope of transfer hydrogenation involving heterogeneous catalysts was restricted to aldehydes or ketones.⁴ Examples of nitrogen heterocycles in such cases were scarce, partly because of catalyst inhibition by the strong coordination of the resulting saturated nitrogen heterocycles.⁵

Inagaki and co-workers previously synthesized bipyridine-periodic mesoporous organosilica (BPy-PMO), in which the 2,2'-bipyridine ligands were regularly arranged and exposed on the pore surface.⁶ Various metal complexes can be directly immobilized on the pore surfaces of BPy-PMO. Such direct immobilization effectively suppresses the unfavorable interactions between the metal catalysts and carrier surfaces, as well as the aggregation of the immobilized metal catalysts. Moreover, BPy-PMO has a large pore size (diameter: 3.8 nm) that enables smooth diffusion of the substrate and product molecules. For these reasons, the catalysts immobilized on BPy-PMO generally show higher catalytic performance as compared to conventional heterogeneous catalysts.^{6,7} Therefore, we prepared a recyclable rhodium catalyst immobilized on BPy-PMO (Rh@BPy-PMO) and employed it in the transfer hydrogenation of diverse unsaturated nitrogen heterocycles.

Results and discussion

Catalyst preparation

Recently, Xu and co-workers revealed that a combination of $[\text{Cp}^*\text{RhCl}_2]_2$ ($\text{Cp}^* = \eta^5\text{-C}_5\text{Me}_5$) and 2,2'-bipyridine as a ligand showed high catalytic activity that was suitable for the transfer hydrogenation of unsaturated nitrogen heterocycles.⁸ They utilized a formic acid/formate buffer that served as a hydrogen donor in H_2O . Inspired by this study, we investigated the transfer hydrogenation of nitrogen heterocycles using a Rh catalyst immobilized on BPy-PMO (Rh@BPy-PMO). Rh@BPy-PMO could be readily prepared by stirring $[\text{Cp}^*\text{RhCl}_2]_2$ with BPy-PMO powder in DMF at 60 °C (Scheme 1). The amount of Rh immobilized on BPy-PMO was easily

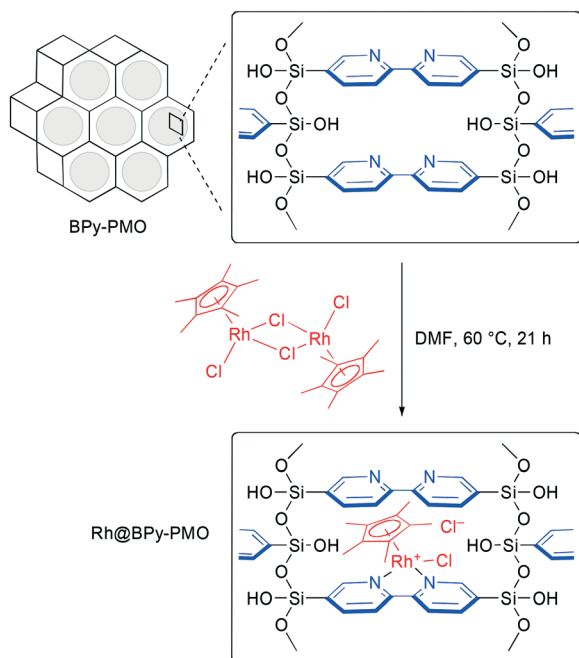
^a Department of Basic Medicinal Sciences, Graduate School of Pharmaceutical Sciences, Nagoya University, Chikusa, Nagoya 464-8601, Japan.

E-mail: yamamoto-yoshi@ps.nagoya-u.ac.jp

^b Toyota Central R&D Laboratories, Inc., Nagakute, Aichi 480-1192, Japan.

E-mail: inagaki@mosk.tytlabs.co.jp

† Electronic supplementary information (ESI) available: Experimental details and characterization data. See DOI: 10.1039/c7cy02167d



Scheme 1 Immobilization of $[\text{Cp}^*\text{RhCl}_2]_2$ on the pore surface of BPy-PMO.

controlled by the initial loading of $[\text{Cp}^*\text{RhCl}_2]_2$. We prepared the catalyst sample with a Rh/BPy molar ratio of 0.06. The corresponding Rh loading was confirmed as 0.20 mmol g^{-1} by energy-dispersive X-ray spectroscopy (EDX, Fig. S1 in the ESI†).

The obtained immobilized catalyst was characterized by ^{13}C cross polarization (CP) magic-angle spinning (MAS) NMR and ^{29}Si MAS NMR spectroscopy. The ^{13}C CP-MAS NMR spectrum of Rh@BPy-PMO clearly showed new signals derived from the Cp^* ligand in the PMO cavity at δ 7.9 and 97.4 ppm, respectively (Fig. S2, ESI†), and these chemical shifts were similar to those of the Cp^* ligand in $[\text{Cp}^*\text{RhCl}_2]_2$ (δ 9 and 97 ppm). The ^{29}Si MAS NMR spectrum of Rh@BPy-PMO showed T^2 $[\text{Si}(\text{OSi})_2(\text{OH})]$ and T^3 $[\text{Si}(\text{OSi})_3]$ signals, but almost no Q^n $[\text{Si}(\text{OSi})_n(\text{OH})_{4-n}]$, $n = 2-4$ signals between -90 and -120 ppm were observed, suggesting almost complete preservation of the Si-C bonds after the immobilization of the Rh complex (Fig. S3, ESI†). Subsequently, the local structure of the immobilized Rh complex was investigated by X-ray absorption fine structure (XAFS) measurements. The X-ray absorption near edge structure (XANES) and extended XAFS (EXAFS) at the Rh K-edge of Rh@BPy-PMO were compared with those of the homogeneous complex $[\text{Cp}^*\text{RhCl}_2(\text{bpy})]$. The XANES spectrum and EXAFS Fourier transform of Rh@BPy-PMO were similar to those of $\text{Cp}^*\text{RhCl}_2(\text{bpy})$ (Fig. S4-S6, ESI†). Curve fitting analysis suggested that the immobilized Rh complex had almost the same electronic state as $\text{Cp}^*\text{RhCl}_2(\text{bpy})$ (Fig. S1, ESI†). These results suggested that the Cp^*RhCl_2 -bipyridine complex was formed successfully over the pore surface of BPy-PMO.

In order to confirm the ordered mesoporous structure of Rh@BPy-PMO, transmission electron microscopy (TEM), X-ray diffraction (XRD) analysis, and nitrogen adsorption-de-

sorption measurements were carried out. The TEM images clearly showed the ordered structure of Rh@BPy-PMO, indicating that the pore channel was maintained throughout the PMO particle (Fig. S7, ESI†). However, the XRD profile showed that the diffraction peak at $2\theta = 1.88^\circ$ that corresponds to a periodic mesoporous structure was lower in intensity compared to that of BPy-PMO. On the other hand, the intensities of the diffraction peaks at $2\theta = 7.54^\circ$, 15.2° , and 22.9° , attributable to the molecular-scale periodicity of the bipyridine ligands in the pore wall, were maintained (Fig. S8, ESI†). The nitrogen absorption isotherm indicated a poorer absorption behavior after the immobilization of the Rh complex as compared to that of BPy-PMO (Fig. S9, ESI†). The BET surface area, pore volume, and pore diameter of Rh@BPy-PMO were $298 \text{ m}^2 \text{ g}^{-1}$, 0.127 cc g^{-1} , and 3.1 nm , respectively.

Optimization of transfer hydrogenation conditions

To establish a viable protocol for the transfer hydrogenation using Rh@BPy-PMO, the reaction conditions were optimized in the case of 3-methylquinoxalinone **1a** (Table 1). In the presence of Rh@BPy-PMO (0.5 mol% Rh), **1a** was heated in a 1 : 1 $\text{HCO}_2\text{H}/\text{HCO}_2\text{Na}$ buffer solution (pH 3.8, 5.0 mol L^{-1}) at 80°C for 2 h to afford the desired product **2a** in 78% yield (NMR), along with 9% of the unreacted **1a** (entry 1). As a side product, small amounts (9% NMR) of *N*-formylation product **2a'** were also detected (δ 1.33 (d, $J = 7.3 \text{ Hz}$, 3H, CH_3), 5.35 (q, $J = 7.3 \text{ Hz}$, 1H, CHMe), 6.93–7.21 (aromatic 4H), 8.63 (s, 1H, CHO)). Next, the influence of buffer concentration and pH was investigated (entries 2–4). The use of a 1 : 2 $\text{HCO}_2\text{H}/\text{HCO}_2\text{Na}$ buffer solution (pH 4.1, 0.6 mol L^{-1}) gave the best result (entry 4). Decreasing the catalyst loading to 0.2 mol% Rh gave a comparable result, and **2a** was isolated in 98%

Table 1 Optimization of transfer hydrogenation conditions

Entry	Rh, mol%	$[\text{HCO}_2^-]^a \text{ mol L}^{-1}$	pH	Yield, ^b %
1	0.5	5.0	3.8	78 ^c
2	0.5	1.3	3.8	89
3	0.5	1.3	4.1	95
4	0.5	0.6	4.1	98
5	0.2	0.6	4.1	(98) ^d
6 ^e	—	0.6	4.1	—

^a The $\text{HCO}_2\text{H}/\text{HCO}_2\text{Na}$ ratios are 2.5 M/2.5 M (entry 1), 0.40 M/0.90 M (entries 2 and 3), and 0.19 M/0.41 M (entries 4 and 5). ^b Yields determined by NMR. ^c *N*-Formylation product **2a'** was obtained in 9% yield. ^d Yields of isolated **2a**. ^e BPy-PMO was used.

yield by silica gel column chromatography (entry 5). BPy-PMO alone did not catalyze the transfer hydrogenation (entry 6).

To gain insights into the catalytic process involving the immobilized catalyst, a hot filtration experiment was carried out.⁶ A mixture of **1a** and the catalyst was heated in a HCO₂H/HCO₂Na buffer solution at 80 °C for 30 min, and the resultant suspension was filtered using a membrane filter (0.1 μm) to remove Rh@BPy-PMO and the solid unreacted **1a**. After adding **1a**, the resultant filtrate was heated at 80 °C for another 23 h, but no noticeable increase in the product yield was detected (Fig. 1). This result indicates that the reaction virtually proceeded at the sites of the immobilized Rh complex on the pore surface of Rh@BPy-PMO. However, ICP-AES measurements of the filtrate revealed a low degree of leaching of the Rh species (<1.2 ppm Rh) from Rh@BPy-PMO. The leached Rh species may be attributed to the [Cp*RhCl₂]₂ precursor adsorbed on the silanol groups (Si-OH) present on the pore surface. It was previously reported that [Cp*RhCl₂]₂ shows no catalytic activity for transfer hydrogenation.⁸

Catalyst recycling experiments

The reusability of Rh@BPy-PMO was investigated by conducting recycling experiments (Fig. 2). After transfer hydrogenation of 3-methylquinoxalinone **1a** under the optimized conditions, the immobilized catalyst was recovered by centrifugation, dried *in vacuo*, and used for the next reaction cycle. On a 6.0 mmol scale, Rh@BPy-PMO maintained high catalytic activity in at least three reaction cycles, affording **2a** in >95% yield. However, the yield of **2a** gradually decreased after the fourth reaction cycle, and the recovery of **1a** increased.

To clarify the nature of the immobilized catalyst after the reaction cycles, the recovered catalyst was inspected by several physicochemical analysis methods. In the ²⁹Si MAS NMR spectrum of the recovered catalyst, no signal was observed at the Q site (Fig. S10, ESI[†]). Thus, the Si-C bond cleavage of

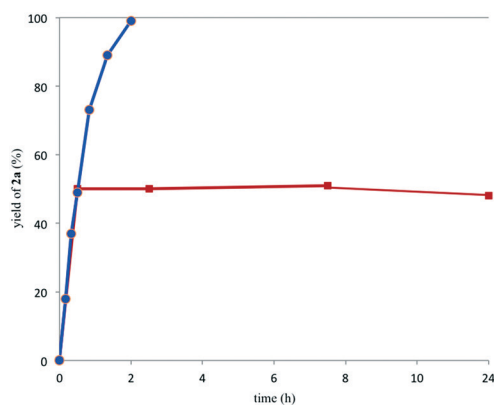


Fig. 1 Progress of transfer hydrogenation of **1a** at 80 °C using Rh@BPy-PMO (red and blue). Rh@BPy-PMO was removed after 30 min (red).

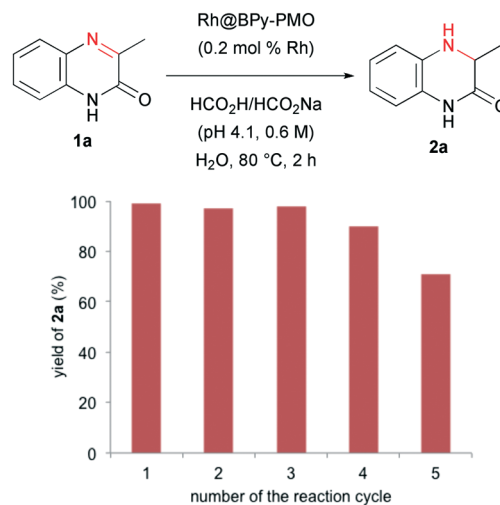
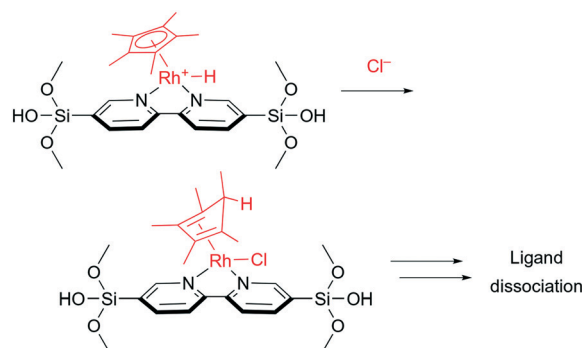


Fig. 2 Catalyst recycling experiments using Rh@BPy-PMO. Isolated yields of **2a**: 1st 99%, 2nd 97%, 3rd 98%, 4th 90%, and 5th 71%.

PMO can be neglected. Moreover, the TEM images of the recovered catalyst showed interference stripes corresponding to the ordered structure of PMO (Fig. S11, ESI[†]). Interestingly, the ¹³C CP-MAS NMR spectra revealed that the intensities of the signals corresponding to the Cp* ligand decreased after the first reaction cycle (Fig. S12, ESI[†]). After the fourth reaction cycle, the Cp* signals completely disappeared, suggesting that the Cp* ligand dissociated during the transfer hydrogenation. Miller and Winkler independently reported that a hydrogen atom is transferred from the Rh center to the Cp* ligand to produce an η⁴-cyclopentadiene complex.⁹ Thus, it is assumed that a similar H-transfer occurred in this study for the immobilized catalyst, and the resultant η⁴-diene ligand dissociated from the Rh center (Scheme 2). Because the catalytic hydrogenation was observed after the Cp* ligand disappeared, bpy-bound Rh hydrides without the Cp* ligand are also catalytically active species, and this fact was not pointed out in the previous study.⁸ In contrast, the ¹³C signals of bpy were observed after the 4th cycle (Fig. S12, ESI[†]), indicating that the pyridine moiety remained intact.



Scheme 2 Plausible mechanism for Cp* dissociation.

Table 2 Transfer hydrogenation of various nitrogen heterocycles^a

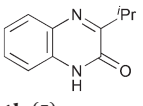
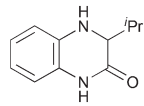
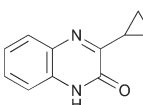
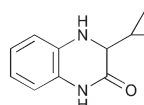
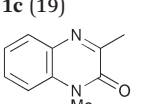
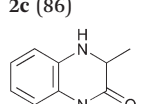
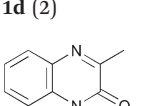
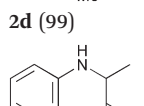
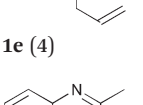
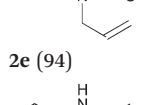
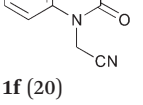
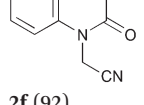
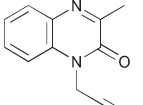
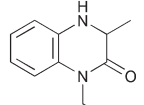
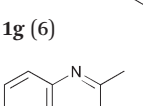
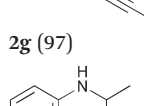
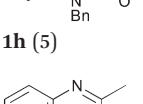
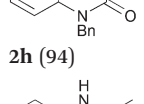
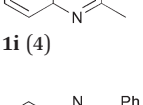
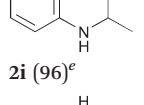
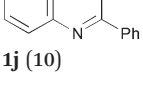
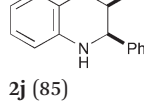
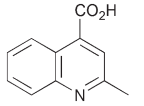
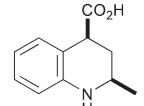
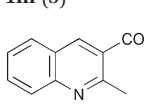
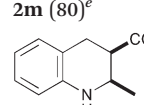
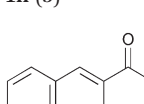
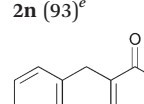
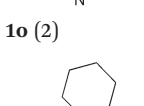
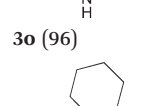
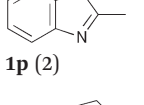
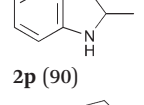
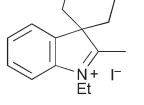
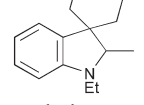
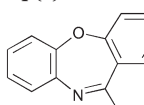
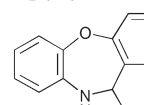
Run	Substrate (time, h)	Product (yield, %)
1 ^b	 1b (5)	 2b (95)
2 ^b	 1c (19)	 2c (86)
3	 1d (2)	 2d (99)
4 ^{b,c}	 1e (4)	 2e (94)
5 ^b	 1f (20)	 2f (92)
6	 1g (6)	 2g (97)
7 ^b	 1h (5)	 2h (94)
8 ^{b,d}	 1i (4)	 2i (96) ^e
9 ^{b,d}	 1j (10)	 2j (85)
10 ^{b,c,d}	 1k (2)	 2k (75)
11 ^{b,f,g}	 1l (24)	 2l (70)

Table 2 (continued)

Run	Substrate (time, h)	Product (yield, %)
12 ^h	 1m (3)	 2m (80) ^e
13 ^d	 1n (3)	 2n (93) ^e
14 ^{b,d}	 1o (2)	 3o (96)
15 ^b	 1p (2)	 2p (90)
16 ^b	 1q (7)	 2q (85)
17 ^b	 1r (24)	 2r (95)
18 ^b	 1s (4)	 2s (84)

^a Standard reaction conditions: **1** (0.3 mmol), Rh@BPy-PMO (0.2 mol% Rh), HCO₂H/HCO₂Na (pH 4.1, 0.6 M, 2 mL), 80 °C.

^b Isopropanol (1 mL) was added. ^c HCO₂H/HCO₂Na (pH 4.1, 0.6 M, 4 mL). ^d HCO₂H/HCO₂Na (pH 4.1, 1.3 M, 2 mL (4 mL for entry 10)).

^e *cis/trans* ratios are 2:1 (entry 8), 15:1 (entry 12), and 7:1 (entry 13).

^f HCO₂H/HCO₂Na (pH 3.5, 1.3 M, 2 mL). ^g 0.5 mol% Rh. ^h HCO₂H/HCO₂Na (pH 4.4, 2.0 M, 2 mL).

Substrate scope

We further investigated the scope of the nitrogen heterocycles for transfer hydrogenation catalyzed by Rh@BPy-PMO. The reaction of 3-isopropylquinoxalinone **1b** was sluggish even under the optimal conditions because of its poor solubility. Thus, 2-propanol was added as a co-solvent. As a result, hydrogenation of **1b** was complete within 5 h, affording the desired product **2b** in 95% yield (Table 2, run 1). In a similar manner, 3-cyclopropyl derivative **1c** was converted into **2c** in 86% yield, wherein the cyclopropyl ring was intact (run 2). *N*-Substituted quinoxalinones **1d–h** were also subjected to transfer hydrogenation, and the corresponding

products **2d–h** were obtained in >90% yields (runs 3–7). Notably, the *N*-allyl, *N*-cyanomethyl, *N*-propargyl, and *N*-benzyl moieties remained intact under the reaction conditions.

The transfer hydrogenation of quinoxalines **1i–k** proceeded efficiently, although a 1.3 M HCO₂H/HCO₂Na buffer solution was required (Table 2, runs 8–10). The reaction of 2,3-dimethylquinoxaline **1i** afforded **2i** in 99% yield with a *cis/trans* ratio of 2:1 (run 8), whereas only the *cis*-isomer of **2j** was obtained in 97% yield from 2,3-diphenylquinoxaline **1j** (run 9). The reaction of indanone-fused quinoxaline **1k** afforded **2k** in 85% yield with the concomitant diastereoselective reduction of the ketone moiety (run 10). The immobilized catalyst also enabled the transfer hydrogenation of substituted quinolines under modified conditions. The reaction of 2-phenylquinoline **1l** was conducted at pH 3.5 under an increased catalytic loading (0.5 mol% Rh), affording **2l** in 70% yield (run 11). The reaction of quinoline-4-carboxylic acid **1m** was performed at pH 4.4 with a 2.0 M buffer solution, affording **2m** in 80% yield and a *cis/trans* ratio of 15:1 (run 12), while the reaction of quinoline-3-carboxylate ester **1n** at pH 4.1 with a 1.3 M buffer solution produced **2n** in 93% yield and a *cis/trans* ratio of 7:1 (run 13). The latter reaction deserves some comments. When the reaction of **1n** was conducted using a buffer of lower concentration (0.6 M), the semireduction product **3n** was selectively generated in 96% yield (NMR) together with trace amounts of **2n** (Scheme 3). This result suggests that primary hydrogenation occurred and that the second hydrogenation of the resultant **3n** was slower because it required protonation of the less electron-rich enamino ester moiety. The same reaction was repeated using the homogeneous catalyst [Cp*RuCl₂]₂/bpy under otherwise identical conditions, and a near 1:1 mixture of **2n** and **3n** was obtained. Therefore, the selective semihydrogenation process is characteristic of the heterogeneous conditions using Rh@BPy-PMO. Interestingly, the reaction of cyclohexanone-fused quinoline **1o** afforded 1,4-dihydroquinoline **2o** as the sole product in 96% yield, even when a higher buffer concentration of 1.3 M was used (run 14). This result suggests that transfer hydrogenation proceeds faster for the nitrogen heterocyclic moiety than for the ketone. This selectivity can be ascribed to the preferable coordination of a softer nitrogen heterocycle than a harder carbonyl oxygen. The carbonyl group of **3o** remained intact because it is incorporated into a vinylogous amide and has low electrophilicity.

In addition to the above six-membered heterocyclic compounds, five and seven-membered heterocyclic compounds were investigated as substrates. In a previous study using a

homogeneous catalyst, the reaction of indole produced the corresponding hydrogenation product with concomitant formylation of the nitrogen atom.⁸ Thus, extra manipulation was required for the removal of the *N*-formyl group. Therefore, indolenine **1p** was subjected to heterogeneous transfer hydrogenation, and protection-free indoline **2p** was directly obtained in 90% yield (Table 2, run 15). In contrast, when indolenium **1q** was used as a substrate, *N*-ethylindoline **2q** was also obtained in 85% yield (run 16). Moreover, benzoxazepine **1r** and benzodiazepine **1s** underwent transfer hydrogenation to afford the corresponding products **2r** and **2s** in 95% and 84% yields, respectively (runs 17 and 18).

Conclusions

We have prepared a rhodium catalyst immobilized on BPy-PMO (Rh@BPy-PMO) by mixing [Cp*RhCl₂]₂ with BPy-PMO in DMF at 60 °C. Rh@BPy-PMO was characterized by several physicochemical analyses, and the local structure of the immobilized Rh complex was observed to be structurally similar to the corresponding homogeneous complex Cp*RhCl₂(bpy). Rh@BPy-PMO could be used as the catalyst for the transfer hydrogenation of unsaturated nitrogen heterocycles in a HCO₂H/HCO₂Na buffer solution at 80 °C. A wide variety of nitrogen heterocycles underwent transfer hydrogenation to afford the products in good yields under modified reaction conditions. The transfer hydrogenation occurred at the site of the immobilized Rh complex on the pore surface of BPy-PMO, as was confirmed by hot-filtration experiments. Rh@BPy-PMO was readily recovered from the reaction mixtures by centrifugation, and the recovered catalyst maintained high catalytic activity up to four reaction cycles of the model substrate.

Conflicts of interest

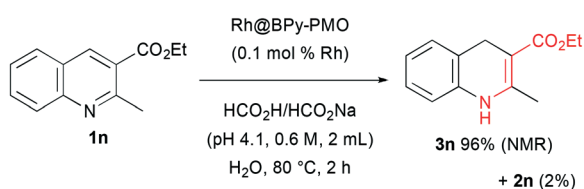
There are no conflicts to declare.

Acknowledgements

This research was supported by AMED (Platform for Drug Discovery, Informatics, and Structural Life Science), ACT-C, from Japan Science and Technology Agency, (Grant Number JPMJCR12Y1), and in part, by a Grant-in-Aid for Scientific Research on Innovative Areas 'Artificial Photosynthesis' (no. 2406) from JSPS. The XAFS measurements were performed at SPring-8 (BL14B2: 2017A1822). The authors thank Dr. Yasutomo Goto (Toyota Central R&D Laboratories, Inc.) for the SEM-EDX analysis and TEM observations.

Notes and references

- (a) J. P. Michael, *Nat. Prod. Rep.*, 2005, 22, 603; (b) J. W. Daly, T. F. Spande and H. M. Garraffo, *J. Nat. Prod.*, 2005, 68, 1556; (c) F. Lovering, J. Bikker and C. Humble, *J. Med. Chem.*, 2009, 52, 6752; (d) V. Sridharan, P. A. Suryavanshi and J. C. Menéndez, *Chem. Rev.*, 2011, 111,



Scheme 3 Semihydrogenation of quinoline-3-carboxylate **1n**.

- 7157; (e) R. D. Taylor, M. MacCoss and A. D. G. Lawson, *J. Med. Chem.*, 2014, 57, 5845; (f) E. Vitake, D. T. Smith and J. T. Njardarson, *J. Med. Chem.*, 2014, 57, 10257.
- 2 Selected recent examples:(a) D. M. Schultz and J. P. Wolfe, *Synthesis*, 2012, 44, 351; (b) C.-V. T. Vo and J. W. Bode, *J. Org. Chem.*, 2014, 79, 2809; (c) M. U. Luescher, K. Geoghegan, P. L. Nichols and J. W. Bode, *Aldrichimica Acta*, 2015, 48, 43; (d) M. Chzanowska, A. Grajewska and M. D. Rozwadowska, *Chem. Rev.*, 2016, 116, 12369; (e) G. J. Tanoury, *Synthesis*, 2016, 48, 2009; (f) M. Shibuya, S. Fujita, M. Abe and Y. Yamamoto, *ACS Catal.*, 2017, 7, 2848.
- 3 Selected reviews:(a) F. Glorius, *Org. Biomol. Chem.*, 2005, 3, 4171; (b) Z. Yu, W. Jin and Q. Jiang, *Angew. Chem., Int. Ed.*, 2012, 51, 6060; (c) D.-S. Wang, Q.-A. Chen, S.-M. Lu and Y.-G. Zhou, *Chem. Rev.*, 2012, 112, 2557; (d) Z. Zhang, N. A. Butt and W. Zhang, *Chem. Rev.*, 2016, 116, 14769; (e) Z.-P. Chen and Y.-G. Zhou, *Synthesis*, 2016, 48, 1769.
- 4 (a) C. Wang, X. Wu and J. Xiao, *Chem. – Asian J.*, 2008, 3, 1750; (b) D. Wang and D. Astruc, *Chem. Rev.*, 2015, 115, 6621.
- 5 (a) A. Kulkarni, R. Gianatassio and B. Török, *Synthesis*, 2011, 1227; (b) L. Tao, Q. Zhang, S.-S. Li, X. Liu, Y.-M. Liu and Y. Cao, *Adv. Synth. Catal.*, 2015, 357, 753; (c) M. Hesticová, M. R. Correro, M. Lenz, P. F.-X. Corvini, P. Shahgaldian and T. R. Ward, *Chem. Commun.*, 2016, 52, 9462; (d) F. Chen, B. Sahoo, C. Kreyenschulte, H. Lund, M. Zeng, L. He, K. Junge and M. Beller, *Chem. Sci.*, 2017, 8, 6239.
- 6 M. Waki, Y. Maegawa, K. Hara, Y. Goto, S. Shirai, Y. Yamada, N. Mizoshita, T. Tani, W.-J. Chun, S. Muratsugu, M. Tada, A. Fukuoka and S. Inagaki, *J. Am. Chem. Soc.*, 2014, 136, 4003.
- 7 (a) Y. Maegawa and S. Inagaki, *Dalton Trans.*, 2015, 44, 13007; (b) N. Ishito, H. Kobayashi, K. Nakajima, Y. Maegawa, S. Inagaki, K. Hara and A. Fukuoka, *Chem. – Eur. J.*, 2015, 21, 15564; (c) X. Liu, Y. Maegawa, Y. Goto, K. Hara and S. Inagaki, *Angew. Chem., Int. Ed.*, 2016, 55, 7943.
- 8 L. Zhang, R. Qiu, X. Xue, Y. Pan, C. Xu, H. Li and L. Xu, *Adv. Synth. Catal.*, 2015, 357, 3529.
- 9 (a) C. L. Pitman, O. N. L. Finster and A. J. M. Miller, *Chem. Commun.*, 2016, 52, 9105; (b) L. M. A. Quintana, S. I. Johnson, S. L. Corona, W. Villatoro, W. A. Goddard III, M. K. Takase, D. G. VanderVelde, J. R. Winkler, H. B. Gray and J. D. Blakemore, *Proc. Natl. Acad. Sci. U. S. A.*, 2016, 113, 6409.